

Consumer-Applicable Retroreflective Microspheres for Use in Polyester Fabrics

By: Omar Abdullah, Megan Lilley, Drew Stasak, Dan Tamayo, Kevin Toula, Lexi Willingham
ENMA 490 Capstone Design

Abstract

Our report will discuss how our team decided upon our design project and the approach we took to meet our design goals. We have designed an assembly of retroreflective barium titanate (BaTiO_3) microspheres immersed in a hot-melt adhesive. The BaTiO_3 microspheres are hemispherically-coated with aluminum and have a radius of 50 μm . Through heating, the assembly can be attached to polyester clothing. If a pedestrian wears clothing with our retroreflective assembly, they will be more readily visible at night to a driver of a car. While some retroreflective products exist, we decided to make a customer-applicable adhesive to have minimal visibility in ambient lighting, but maximal visibility at night. This type of product is not currently on the market. The design approach included materials selection, process formation, ray tracing, and calculations to show how our retroreflective adhesive would function in accordance with the light given off by car headlights. The optimal divergence angle for our scenario was calculated to be 0.697 degrees.

Motivation

Being a student at the University of Maryland over the past couple years has meant experiencing many changes aiming to improve pedestrian safety. Sadly, these changes were not preventative measures, but the result of the tragedies our community has felt with the hopes that any future accidents would be avoided. Pedestrian injuries due to automobiles occur about every eight minutes, with the majority of these happening at night [1]. It is extremely difficult to notice people walking along or near the side of the road at nighttime until the car is right behind them, when it may be too late to avoid an accident. The most difficult times to see a pedestrian at night are when there are no sidewalks, crosswalks, or streetlights. In these cases, it would be extremely helpful and possibly life-saving if pedestrians were visible to a driver at a safe distance. Retroreflective technology would be beneficial in these situations because the clothing would reflect when a light was shining on it.

Retroreflection is a phenomenon in which a material will reflect light parallel back to its source. If retroreflective materials were used in clothing, when a car's headlight hits the person, they would become noticeable to the driver at a safe distance away. This would potentially lead to fewer accidents between cars and pedestrians.

Materials Science and Engineering Aspects

This project required many skills we acquired throughout our time as undergraduate students in the Department of Materials Science and Engineering. We used knowledge in the areas of physics, chemistry and engineering, most importantly focusing on polymers, optics and processing techniques. For our design, we chose the

materials for our microsphere and hemispherical coating based on optical properties like index of refraction and reflectivity. Later, we needed a knowledge of polymers in order to choose our adhesives based on temperature properties and bonding strengths. We considered the strength of adhesion of the chosen hot melt polyurethane to both the microspheres and the polyester fabric to ensure the durability of our product. One of the processing techniques that we utilized in our manufacturing design was sputter deposition. Lastly, we used ray tracing and calculations to simulate the retroreflection of our chosen microspheres. This was an important aspect of our design, as part of our goal was to maximize the light reflected back into the eyes of the driver.

Previous Work

Currently, there are two main categories of retroreflective clothing. The first category is fluorescent clothing with retroreflective strips. This type of clothing is commonly worn by construction and other roadside workers as well as hunters. Many people are not inclined to wear this type of clothing unless it is required, due to its relatively unappealing visual appearance. The fluorescent colors are bright and noticeable during the day; however, at night they do not have the same effect. Although bright colors are more noticeable at night than dark colors, visibility problems still result as they would with any normal clothing. The retroreflective strips are needed in order for the clothing to be visible at night. The second category of retroreflective clothing is athleticwear. This type of clothing is designed so they are not constantly reflecting light, only when light with enough light intensity, like a car's headlights compared to ambient lighting inside a room, is shining on the article of clothing. A disadvantage of these types of clothes are their very limited style and select consumer market. Since these retroreflective clothes are fairly new to the market, not many companies offer them as options, so these clothes tend to be expensive. The basis of our design project is the combination of the effects of these clothing options. Our goal is to have the retroreflectivity of the first category with the aesthetic appearance of the second category.

The retroreflective materials currently used are glass microspheres, although they can be other shapes such as prismatic cube-corners [2]. To increase the retroreflectivity, the glass is sometimes coated. Commonly used materials are barium titanate coated in aluminum [3]. 3M™ Scotchlite is the most well-known and widely used retroreflective material that uses this technology. The current technology for the athletic wear is similar, but the athletic companies have found ways to incorporate the retroreflectors in large portions covering most or all of the article of clothing as opposed to 3M™ Scotchlite which tends to be used in small, strategic areas.

Design Goals

The desire to improve pedestrian safety at night led us to look for a way to improve pedestrian visibility to a driver in a car. In order to accomplish this, we set out to create a retroreflective adhesive that a customer can apply to their own clothes easily. The retroreflective material must not be highly visible in natural lighting to differentiate our design from the current retroreflective material available. The application of the

retroreflecting material should have a minimal effect on the clothing's look and feel; the product is intended only to be seen when exposed to a direct, intense light source.

Technical Approach

Our first objective was to meet our design goal; create a consumer applied product, seen below in Figure 1, that layers over top clothing and is inconspicuous in daylight, but makes the wearer easily visible when illuminated by the headlights of a car from a certain distance. Using our goals as guidelines, we determined how we would design the product to meet our desired criteria. In order to meet the main objective, visibility under illumination by headlights, we decided to use retroreflective microspheres, which are optically transparent microspheres that are hemispherically-coated with a metal. Retroreflectors oriented perpendicular to the clothing will reflect the light back to the source, in this case the driver of the car, in a non-diffuse manner. This allows for a large amount of light to return in the direction of the light source, making the wearer of our product visible to a driver while also ensuring that the user does not "glow" at all other times. There would be no unwanted retroreflectivity because most ambient light sources come in at an angle not parallel to the average person's eyes. After determining that the person would not glow as a result of the optical reflectance of the material, we next needed to ensure that the retroreflectors themselves would not stand out. Since we are using microspheres, they are much too small to be visible from a few feet away. We decided that we could use a transparent adhesive to attach the microspheres and use processing to leave only this adhesive between the microspheres and the fabric, making the retroreflectors inconspicuous as we desired. The last goal we needed to satisfy for the product was to make it consumer-applicable. Relating to an earlier objective, the microspheres needed to be oriented by the end of the application process. The required orientation is for the metallized side to be facing in the clothing, while the bare BaTiO₃ side is facing away from the clothing. If the microspheres are not oriented properly, they will not retroreflect in the desired manner. We decided to accomplish the orientation by sputtering a metallic film on the particles, then using a hot-melt adhesive to "pick-up" the metallized side of the microspheres. In addition, we use a temporary adhesive film on the bare BaTiO₃ sides of the microspheres to ensure the microspheres do not re-orient during application to the shirt. The orientation and processing are further described in the "Manufacturing and application" section of the paper.



Figure 1: A diagram of the product received by the consumer

Materials Selection

Microspheres

Once the end product and goal were decided, we needed to select our materials. For the microspheres, our main criteria was to find a material with optimal

retroreflectivity. There are two main types of retroreflector shapes, cube corners and spheres. Cube corners are best manufactured in rows, but we chose to use microspheres in order to have individual particles that would be less visible. Thus we needed to choose a material for the sphere. To determine what materials work best as retroreflecting spheres we equated the scenario to a ball lens with an effective focal length (EFL) of radius r . Using that condition to determine EFL, we solved Equation 1.

$$EFL = \frac{nr}{2(n-1)} \quad \text{Equation 1}$$

$$r = \frac{nr}{2(n-1)}$$

$$1 = \frac{n}{2(n-1)}$$

$$2(n-1) = n$$

$$2n - n = -2$$

$$n = 2$$

As can be seen by Equation 1, a perfect retroreflector would have an index of refraction of 2; however, this would not be ideal since perfect retroreflection would mean only the light that undergoes scattering and aberration would reach the driver's eyes, while the majority of the light is reflected back to the headlights. Thus, using a material that has an index of refraction near, but not exactly at 2 would be ideal. Based on research, we found that barium titanate, BaTiO_3 , would be an ideal material for our design purposes. Barium titanate is an optically transparent material with an index of refraction of 1.93 and is a commonly used retroreflective microsphere material in industry, indicating that the potential for scale-up would be possible [4].

Next, we chose the material that will serve as the reflective coating for the microspheres. Our criteria for this was that it must be possible to apply it to the microspheres and be able to serve as a reflective surface. Given this criteria, a variety of metals are potential materials. We chose aluminum because it would meet the criteria at a relatively low cost. We chose to use cost as our third factor since cost is always an important factor in industry.

Adhesives

The next step was to choose an adhesive that would bond the microspheres to polyester clothing. For this, we chose an ester based polyurethane hot-melt adhesive, specifically GLUETEX UKF 438. Polyurethane is already used for sealing fabrics, and it can withstand washing/drying cycles in a home washer/dryer [5]. The aluminum coating on the microspheres can be sufficiently bonded to the ester-based polyurethane [6]. In addition, the hot-melt adhesive must be applied at temperatures that consumers have access to and do not degrade the fabrics. The polyurethane is suggested to be applied between 125 °C and 150 °C. Since polyester already has a suggested ironing temperature of 148 °C, the polyurethane application temperature will not degrade polyester fabric [6]. The process on the consumer end is simple because for the application process the consumer only has to use an iron to melt the film onto the

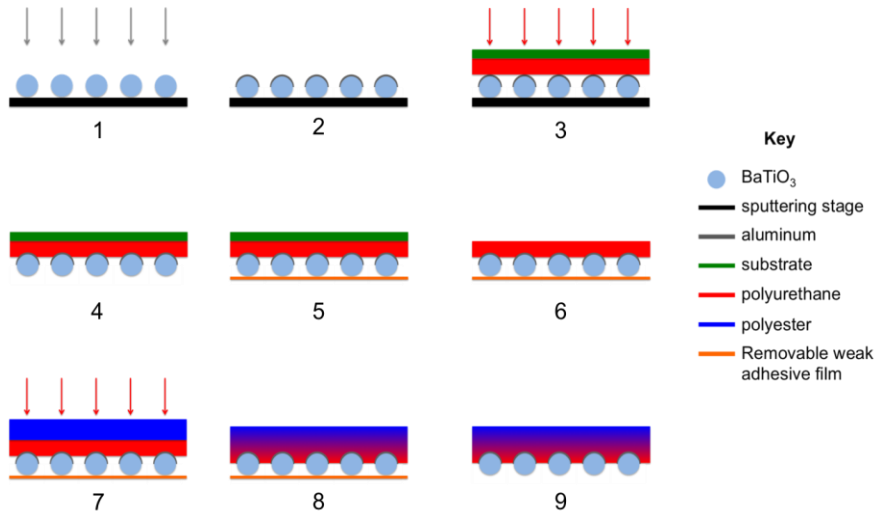
clothing, let it cool, and peel off a temporary adhesive layer.

When we incorporated the temporary adhesive layer into our design, our need for an easily removable adhesive with a very high resistance to heat led us to choose a Kapton® polyimide film and silicone adhesion. The temperature use range given in a technical data sheet given by 3M™ is -73°C to 260°C [7]. Although the strength of adhesion is only given for adhesion between the polyimide and steel, the technical data sheet claims that their tape is easily removable and the high temperature performance helps reduce adhesive transfer. The fact that the polyimide is easily removable would prevent any pieces of the adhesive from remaining on the microspheres and interfering with the retroreflection. The only other confirmation of this choice that we need is a comparison to the strength of adhesion between the the hot melt and microspheres. Given the fact that the strength of adhesion is weaker between the polyimide film and the BaTiO₃, the removal of this film will not affect the microsphere attachment or orientation [7]. We could not collect enough data on the interfacial energy between the polyimide film and the BaTiO₃ microspheres to calculate the strength of adhesion using JKR theory, so this would have to be determined in the prototype and testing phase.

Manufacturing and Application

Once we chose our materials, we moved forward with designing a manufacturing process. To begin the process, the barium titanate microspheres would be placed on the stage of a sputtering apparatus. The microspheres would then be sputter deposited with aluminum, as seen in step 1 of Figure 2. The directionality of the sputtering process would leave the microspheres hemispherically coated, as only half of the sphere would be exposed to the sputtering system, shown in step 2. Polyurethane is then placed on top of the microspheres, attached to a metal substrate to keep the polyurethane and microsphere film smooth, seen in step 3. In step 4, heat is applied to bind the microspheres and polyurethane together. After the hot-melt adhesive cools down, the assembly is lifted and has a polyimide film placed across the side with uncoated, exposed microspheres, as seen in step 5. In step 6, the metal substrate is removed and the product is no longer in the manufacturing phase; it is ready for consumer application.

Beginning the application process, step 7 shows the consumer applying the coating to their clothes using an iron-on method, with the polyurethane side facing the clothes. The heat from a household clothing iron melts the polyurethane into the substrate, in this case the clothing. Upon cooling, the shirt and microsphere assembly are now bonded, shown in step 8. The last step is to remove the polyimide film, seen in step 9, as it is no longer needed to keep the microspheres oriented.



In order to ensure that the light will be retroreflected back to the driver's eyes, we needed to calculate the divergence angle necessary for our design to be valid. Using the situation shown in Figure 3 we can see what angles need to be calculated in order to determine the divergence angle. The divergence angle needed is the sum of θ_i and θ_o .

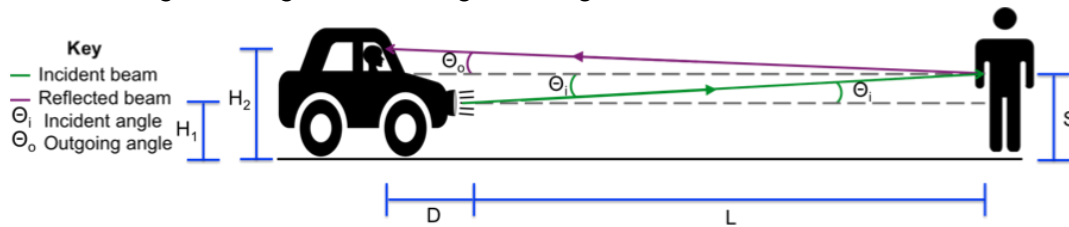


Figure 3: Diagram displaying the ray of light and how it would need to reflect in order to reach the driver's eyes.

The angles can then be calculated using Equations 2 and 4, leading us to Equation 6 to show divergence angle θ_D .

$$\tan(\theta_i) = \left(\frac{S-H}{L}\right) \quad 2$$

$$\theta_i = \tan^{-1}\left(\frac{S-H}{L}\right) \quad 3$$

$$\tan(\theta_o) = \left(\frac{I-S}{L+D}\right) \quad 4$$

$$\theta_o = \tan^{-1}\left(\frac{I-S}{L+D}\right) \quad 5$$

$$\theta_D = \tan^{-1}\left(\frac{S-H}{L}\right) + \tan^{-1}\left(\frac{I-S}{L+D}\right) \quad 6$$

By using the data shown in Table 1 the necessary divergence angle can be calculated for a person based on average heights, gender, age, and type of vehicle. For our purposes, age 5 to 12 is a child and we are assuming that the light is interacting at a height three quarters a way up the body [8]. The different scenarios were then plotted in figure 4. Length L was found to be 344 feet, or 104.85 meters [9]. We determined this length from the average stopping distance for an automobile traveling at 65 mph, since it is unlikely for pedestrians to travel on roads where automobiles are traveling in excess of

65 mph [9]. Based on Figure 4 we can see that the aberration decreases as the microsphere radius increases. Based on the resulting data, the maximum angle of divergence is 0.697 degrees at furthest detection distance, indicating that our selected material must have a divergence angle of 0.697 degrees or less. We are calculating based off of stopping distance because that is the range at which the pedestrian must be seen in order to prevent an accident. It should be noted that while the angle of divergence may exceed the divergence of our chosen microsphere material, it is acceptable because at distances beginning near 125 feet, the pedestrian is at a range where they are somewhat visible by the driver without the aid of the retroreflectivity.

Table 1: A display of average heights based on the age and gender of the pedestrian, as well as average values for the type of vehicle. All measurements in meters.[10][11][12].

Height	Adult Male	1.320165
	Adult Female	1.21539
	Child Male	1.007745
	Child Female	1.008698
Driver Eye Distance	Car	1.928333
	Truck	1.34
Driver Eye Height	Car	0.645
	Truck	0.816
Headlight Height	Car	0.645
	Truck	0.816

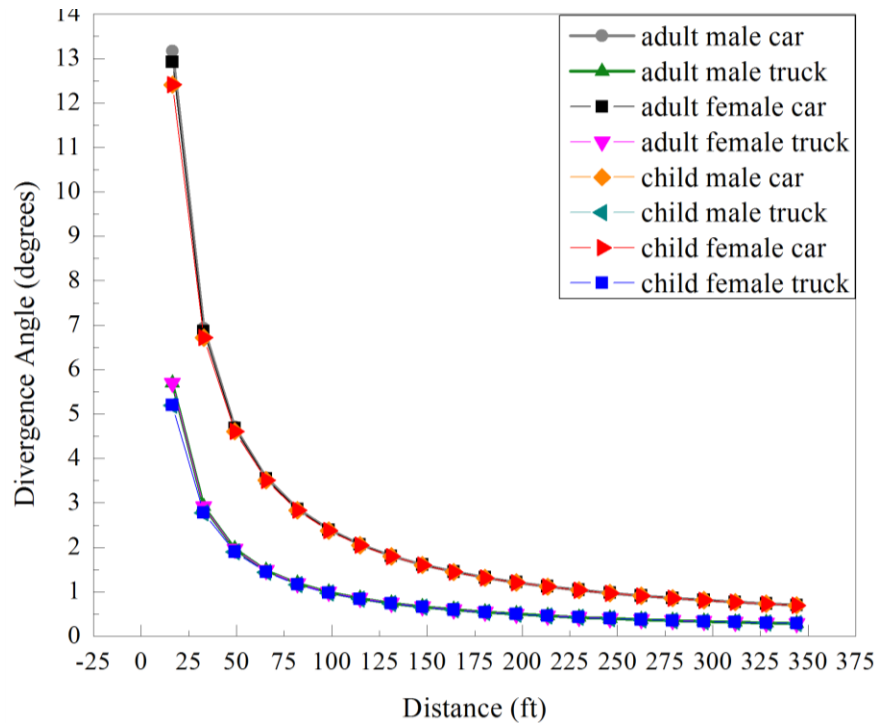


Figure 4: A graph of the divergence angle for various cases with respect to the distance between the pedestrian and the front of the vehicle.

Next we will clarify the optimal wavelength for later calculations. This wavelength will be determined by what the receptor, the eye, is most sensitive to. The eye has four types of receptor cells in it; blue cones, green cones, red cones, and rods, each of which work optimally for specific wavelengths [13]. Rods are optimized for motion detection and low-light vision, and while they may appear to be the ideal receptor for our low-light conditions, they require an activation period in darkness which they can not achieve in the presence of headlights [14]. This leaves cones as the main receptor cells to determine the optimal wavelength. A graph of the normalized sensitivities over the visible spectrum of wavelengths for each cone is shown below in Figure 5. It can be noted that the red cones actually peak in the wavelength of yellow light, and combined with the intensity of the green cone spectrum, this results in green light wavelength of 550 nm being the optimal wavelength for our use in calculations.

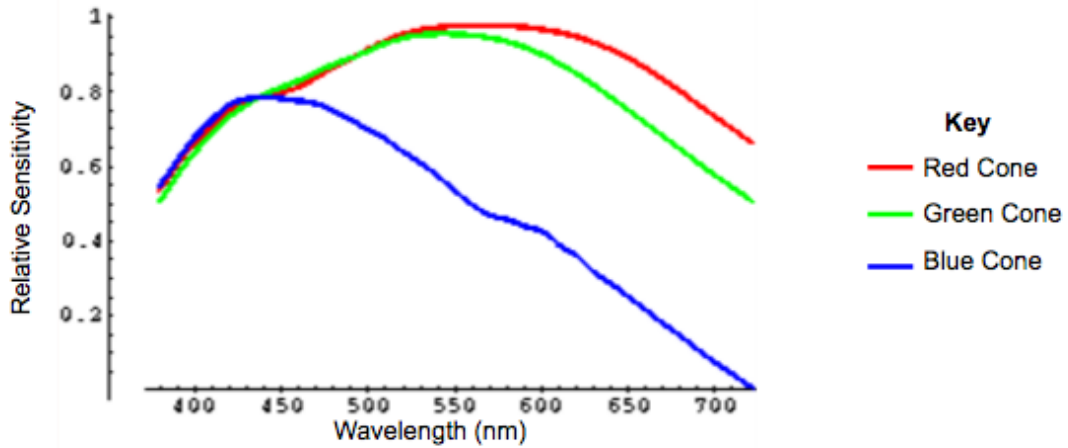


Figure 5: A graph of the normalized sensitivity of blue, green, and red cones over the visible spectrum [13].

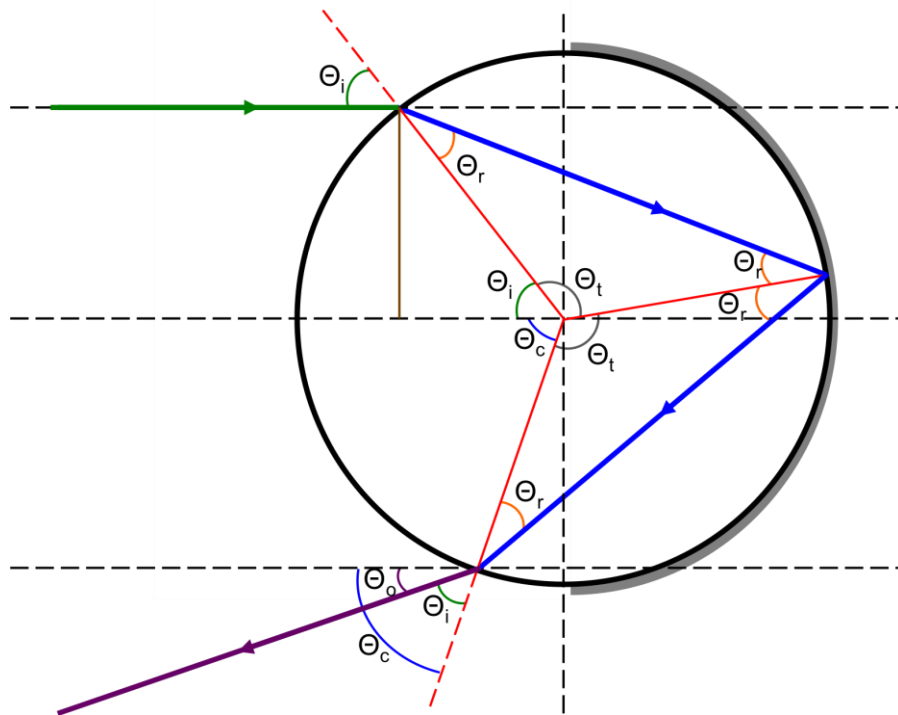


Figure 6. Ray tracing diagram

The amount of light retroreflected back to the driver's eyes from each microsphere can be approximated using the equations below. These equations assume the light will be entering the microsphere as parallel rays. These equations were derived from Snell's law as well as the geometries shown in Figure 6 above. Equation 7 is used to find the refracted angle of the light ray when a parallel beam of light hits the sphere at an incident height based upon the radius and index of refraction of the sphere.

$$\sin^{-1}\left(\frac{h_i}{R}\right)/n = \theta_r \quad \text{Equation 7}$$

Equation 8 uses the refracted angle found with Equation 7 to find the odd angle of the isosceles triangle created between the three points of the location the incident ray hit the sphere, the location the refracted ray hit the back of the sphere, and the center of the sphere. This triangle is then mirrored about the axis of reflection to find the location where the ray will leave the sphere.

$$180 - 2\theta_r = \theta_t \quad \text{Equation 8}$$

Equation 9 uses the incident height with which the ray hits the sphere to calculate the angle the ray is tilted from the normal of the sphere.

$$\sin^{-1}\left(\frac{h_i}{R}\right) = \theta_i \quad \text{Equation 9}$$

Equation 10 combines the angles found in Equations 8 and 9 to find the angle from the center of the sphere to the point at which the ray leaves to the parallel.

$$360 - 2\theta_t - \theta_i = \theta_c \quad \text{Equation 10}$$

Equation 11 combines the angles found in Equation 9 and 10 to find the angle with which the leaving ray creates with the parallel.

$$\theta_c - \theta_i = 360 - 2(180 - 2(\sin^{-1}\left(\frac{h_i}{R}\right)/n)) - 2\sin^{-1}\left(\frac{h_i}{R}\right) = \theta_o \quad \text{Equation 11}$$

Equation 11 was then graphed in Figure 7 using Matlab where both the incident height and the refractive index of the material of the sphere were varied. The range for the incident height was set from zero, the center of the sphere, to the radius of the sphere. The range for the index of refraction of the material was set from 1.83 to 2.03 to cover a range around the index of refraction of BaTiO₃.

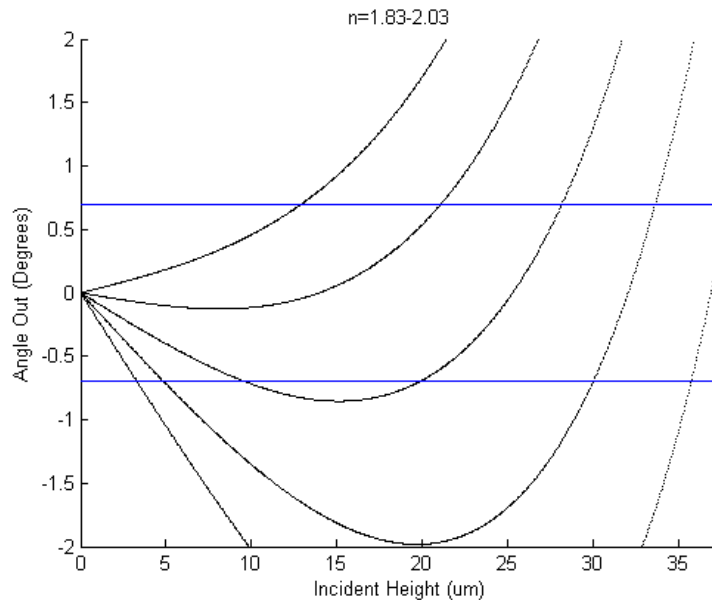


Figure 7. The angle the exiting ray leaves from the sphere with respect to the parallel as a function of the incident height of the incoming ray. The blue line is the optimal angle of reflection at a distance of 344 ft. The refractive index changes by 0.05 with 1.83 being the lowest line and 2.03 being the highest line.

The reflectance and transmittance of the microspheres were determined using Fresnel equations. The Fresnel equations determine these characteristics based upon the differing indices of refraction of the two transparent media by relating the polarization of the waves to the plane of incidence [17]. The angle of incidence ranges from -90° to 90° since half of the microsphere will be exposed for light to enter; however, for our purposes we only needed to do calculations for 0° to 90° due to symmetry. To find the angle at which the light is refracted, we used Equation 12, Snell's Law.

$$n_1 \sin \theta_i = n_2 \sin \theta_t \quad \text{Equation 12}$$

After finding the transmittance angles, the reflectance and transmittance coefficients for both s- and p-polarized light were calculated using the Fresnel equations below. S-polarized light is perpendicular to the interface and p-polarized light is parallel to the interface.

$$r_{\parallel} = \frac{\tan(\theta_i - \theta_t)}{\tan(\theta_i + \theta_t)} \quad \text{Equation 13}$$

$$r_{\perp} = -\frac{\sin(\theta_i - \theta_t)}{\sin(\theta_i + \theta_t)} \quad \text{Equation 14}$$

$$t_{\parallel} = \frac{2 \sin(\theta_t) \cos(\theta_i)}{\sin(\theta_i + \theta_t) \cos(\theta_i - \theta_t)} \quad \text{Equation 15}$$

$$t_{\perp} = \frac{2 \sin(\theta_t) \cos(\theta_i)}{\sin(\theta_i + \theta_t)} \quad \text{Equation 16}$$

We were able to use simplified versions of these equations because BaTiO_3 is non-magnetic so the permeabilities cancel in the original equations and can be simplified with Snell's Law into Equations 13-16 above [15]. The relationship between these coefficients and the incidence angle can be seen in Figure 8 below.

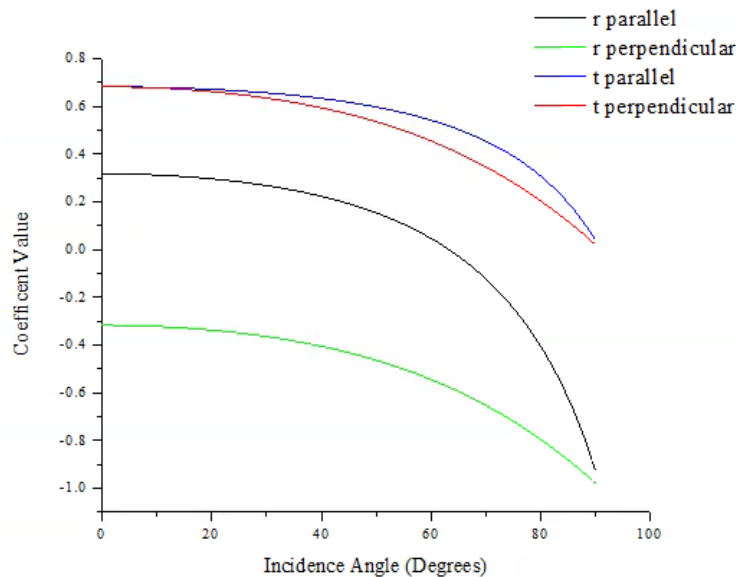


Figure 8: Fresnel Coefficients

The amount of light reflected, our main concern, is determined by squaring the reflection coefficient values. Since our light source is unpolarized, the total amount of light reflected can be found by taking an average of the reflectance in the parallel and

perpendicular directions. The transmittance can be found by subtracting the reflectance from unity. The reflectance for each incidence angle is shown in Figure 9. The transmittance at each angle would be a mirror image in the x-axis of the graph for reflectance. Although the reflectance at angles less than approximately 80° is poor, the light will be coming in from multiple angles since it is not a singular ray of light so there will be varying degrees of reflectance out of each individual microsphere giving a satisfactory reflectance overall.

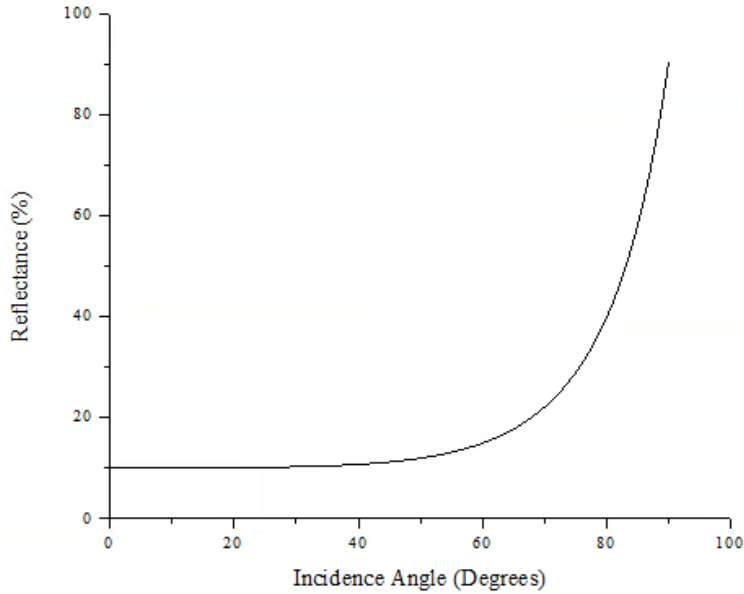


Figure 9: *Light Reflectance*

One concern that arose from using a glass lens was the effect of chromatic aberration. Chromatic aberration is how the index of refraction of the glass changes based on different wavelengths of light [16]. The index of refraction of a material will be greater for shorter wavelengths. Normally, this type of aberration is a relationship between the two different curvatures in the lense, and it is corrected by combining lenses that have different shapes, curvatures, or indices of refraction. However, our project’s design is only based on a single piece of the BaTiO₃ with equal radii of curvature that will act as the lens, and the BaTiO₃ is acting as a retroreflector, not an image forming lens, so the above corrections do not apply. Therefore, we have only demonstrated the relationship and acknowledged that it will affect the diffraction of the light entering the microspheres depending on the corresponding index of refraction.

The relationship between index of refraction and wavelength is based on the Sellmeier Equation, Equation 17 [18].

$$n^2 = A + \frac{B\lambda^2}{\lambda^2 - c} + D\lambda^2 \quad \text{Equation 17}$$

The variable constants A, B, C, and D depend on the material and are determined through experimental fits. The corresponding values of A, B, C, and D for BaTiO₃ are 3.0584, 2.27326, 0.07409, and -0.02428 respectively [18]. This data is given for BaTiO₃ in general and not the specific BaTiO₃ we would have purchased had we decided to prototype our design. The BaTiO₃ microspheres we would have purchased have an index of refraction of 1.93. There are a range of possible indices of refraction that BaTiO₃ can have based on the manufacturer. We used Equation 17 to give the general trend of how chromatic aberration will have an effect on the index of refraction as it changes with wavelength. The relationship can be seen in Figure 10 with specific wavelengths highlighted for the visible light spectrum ranging from 380 nm to 750 nm, or 0.38 μm to 0.75 μm. For violet and red wavelengths, the most extreme values were used. The wavelengths highlighted for blue, green, yellow, and orange light are an average of the range of wavelengths in that given color spectrum. The calculations were done using units of micrometers for wavelengths as opposed to nanometers. When using numbers in nanometers, the equation becomes invalid because the result n^2 is equal to a negative number, since the numbers in nanometers are too large. When calculated in meters, the wavelengths are on a small order of magnitude of 10^{-7} , and the calculation cannot distinguish a varying relationship, so the unit of micrometers had to be used.

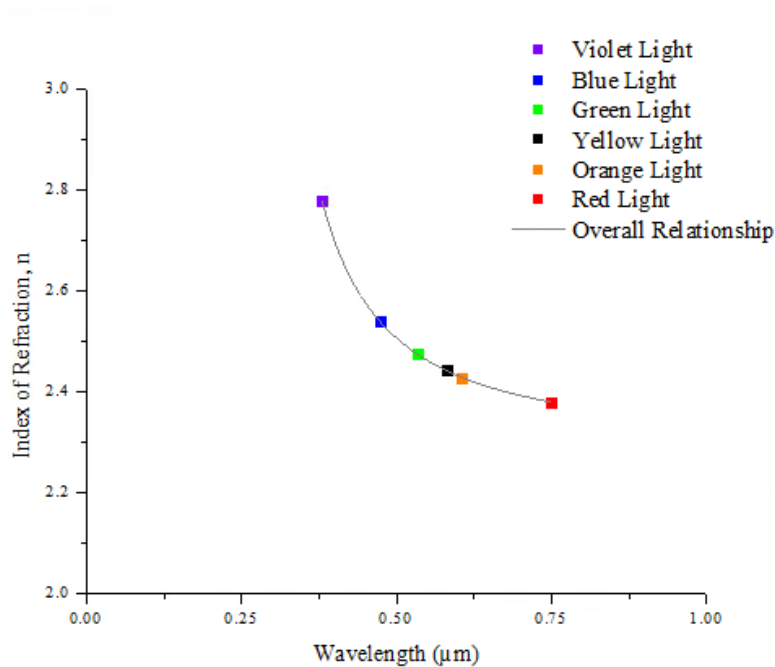


Figure 10: *Chromatic Aberration Effect on Index of Refraction*

Spherical aberration is another important factor to our design. Based on advice from Dr. Phaneuf, we focused on a specific term of the spherical calculations. Using Seidel's equation for for the third-order term of spherical aberration we were able to derive Equation 18 [18].

$$S = \frac{2(n-1)}{R^3 \times 8}$$

Equation 18

Using that equation we then calculated the aberration as it varies with radius, shown below in Figure 11. It is clear that the aberration decreases as the microsphere radius increases. Furthermore it should be noted that the scale for aberration is logarithmic, indicating that the decrease in aberration falls off sharply near 50 microns.

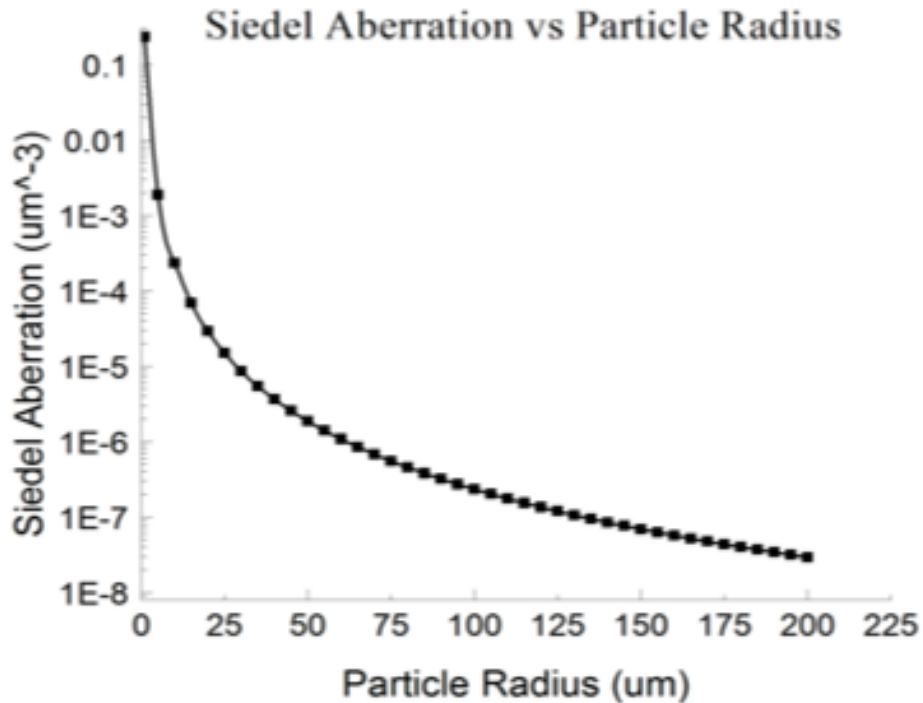


Figure 11: A graph showing how spherical aberration decreases as sphere radius increases.

An additional point of concern was the potential loss in intensity due to scattering effects. Of particular importance is the effect as the size of the particles change. Among the most elegant and powerful methods of calculating the effect of particle size on scattering angles and intensity losses is the Mie solution to Maxwell's equations [19]. Mie theory transforms the incident and scattered fields into spherical vectors, which form the general solutions for spherical harmonic electromagnetic fields. The coefficients of this transform, as well as the extinction and scattering coefficients may be calculated, which can be utilized to determine the absorption, scattering and extinction cross sections.

There are a large number of programs and plugins that perform Mie scattering calculations in a variety of programming languages. Due to the time constraints of this project, MiePlot created by Philip Laven was selected as the scattering modeling program of choice.

Figure 12 below demonstrates the effect of increasing particle radius on the resulting scattered power. This increase in scattering is due to the greater cross

sectional areas of the larger particles, which increases the relative intensity each bead scatters.

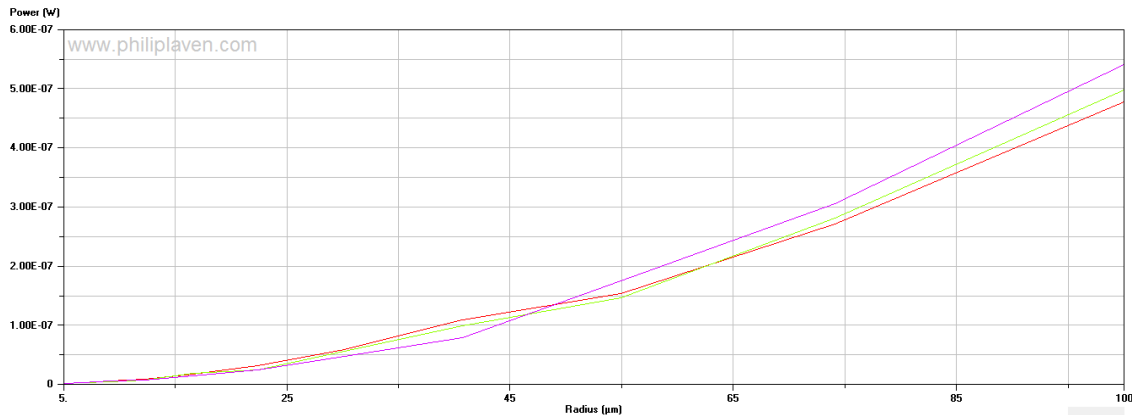


Figure 12: Mie theory plot demonstrating the effect of increasing radius size on the scattered power.

As can be seen in Figure 12, this effect has a nearly linear rate of increase, as such selecting to minimize the spherical aberration which demonstrates a $1/R^3$ will yield the most significant change in the particle performance. An ideal compromise lies prior to the exponential increase in the losses for spherical aberrations. This will serve to minimize both the scattering losses, as well as the spherical aberrations, a location found at approximately 50 microns.

Durability

We have also investigated how the BaTiO_3 particles will remain intact with the polyurethane adhesive due to environmental conditions. One of the most taxing environments which our particles will endure is the washing machine. In addition to be submerged in water containing detergents the particles will also be subject to mechanical forces from the rotation of the washing machine drum. Depending on the orientation of the particle these forces can act in both compression (if the particles are pressed against the drum) and tension (if the particles are over one of the water diverging holes). The amount of centrifugal force exerted on the particles by the washing machine can be found from the dimensions of the washer drum, the rotational speed of the washer, and the mass of the particle. Common specifications of consumer available washing machines have a radii range from 22 to 30 cm and rotational speed range from 1200 to 1800 rpm. The mass of the particle (2.51×10^{-5} g) was found using the radius of the particle (150 µm) to get its volume, due to its spherical shape, and multiplying by the density of BaTiO_3 (6.02 g/cm^3). Centrifugal force was then be calculated using Equation 19.

$$F_c = m_{particle} * 1.12 * R_{washer} * \left(\frac{rpm_{washer}}{1000}\right)^2$$

Equation 19

For the high range of washing machine specifications the force was calculated to be

0.02734 N. This force was then roughly converted to a pressure using the cross sectional area of the disk as an estimate of the amount of surface area the polyurethane adhesive which is attached to the sphere and polyester with Equation 20.

$$P_{washer} = \frac{F_c}{\pi(R_{particle})^2} \quad \text{Equation 20}$$

This pressure was calculated to be 0.386 MPa at a maximum exerted by the washer on the particles. Looking at the material properties for ester based polyurethane adhesive given in CES EduPak the range of compressive and tensile strength ranges from 18-55 MPa. The polyurethane adhesives' compressive and tensile strength is well above the maximum pressures that will be exerted on the adhesive from the wash cycle, which means it is suitable for our application.

Prototype

Halfway through the project, our team decided we would not go forward with prototyping. Instead, we would focus all of our efforts on ensuring our design is as well-thought out and accurate as possible in the time allotted. We have, however, chosen the specific materials, mentioned previously, we would have used if we had decided to prototype and test our design.

Ethics and Environmental Impact

One large ethical concern for this project is that our project centers around the use of microbeads (microspheres). There has been concern in recent years as to the safety using microbeads for products around the human body as well as what happens to the microbeads after use. Specifically, plastic microbeads have been banned [20]. The concern for the use of the microbeads around the body is the size of the microbeads being smaller than the pore size of human skin. Skin pore size is approximately 0.02 μm [21]. The microspheres we have based our design on are 50 μm in diameter, so we are not concerned with the microspheres getting lodged in the skin.

Our secondary concern is how loose microspheres may interact with the environment. Often, microspheres are not biodegradable, so they can pollute the environment, water supplies, and wildlife [20]. If the consumer is not careful, it is possible for the microspheres to dislodge and enter water sources and the rest of the environment. Had we decided to test the microspheres in this class, we would have needed to be careful to minimize the amount of microspheres that dislodge from the adhesive. We can combat this issue by implementing water filters to prevent the microspheres from entering both the environment and back into public water supplies.

Intellectual Merit

In terms of scientific and engineering merit, this project studied the mechanical and optical properties of retroreflective microspheres in a polymer matrix, applicable by the consumer. There is limited retroreflective technology available on the market, for that reason, the methodology is trademarked and not publically shared. As such, on a scientific level, this project, if successful, will serve the dual purposes of drawing

attention to the state of retroreflective research in order to generate interest and promote future projects.

In the initial stages of the project, the group gathered information for material selection through networking with professionals in addition to researching and modeling of the optical properties of BaTiO₃ and the adhesive properties of the polyurethane. Gaining knowledge of modeling techniques will be beneficial in pursuit of further academic and industrial goals where modeling is an increasingly useful tool with the continual increase in computer power. Finally, the group acquired skills in experimental design.

Broader Impact

By far the largest impact that our design can offer is the improved safety of pedestrians. The goal of our project is to design a product that makes pedestrians more visible by drivers from a further distance during low-light conditions. This would allow pedestrians to travel safer at night, especially in areas where there may not be roadside lighting, in areas lacking sidewalks, or if the clothing makes it difficult for the pedestrian to be seen. By making pedestrians more visible they in effect become safer, and consequently this design has a positive impact on society. Our project idea is also unique in that the microsphere assembly is intended to be inconspicuous and consumer-applicable. If fabrication of our design was successful, this would introduce new potentials in retroreflective fabric technology.

Results and Discussion

Our results are completely based on our design calculations and modelling. Although we did not prototype, we have decided on the specific materials we would have used. Based upon the materials described earlier in this paper, we have checked that the properties are compatible with each other. Our design process relied heavily on computational analysis. We have finalized the manufacturing and application processes, portrayed previously in Figure 2. In our specific case, the angle of divergence necessary for retroreflection to be a success was calculated to be 0.697 degrees. Using ray tracing techniques, we proved that BaTiO₃ with an index of refraction of 1.93 is the best choice because it gives angles of reflectance closest to the optimal angle of reflection at a stopping distance of 344 feet. Using Fresnel coefficients, we calculated the reflectance at each incident angle. We studied chromatic aberration and found that the index of refraction decreases as the wavelength of light increases. With regards to spherical aberration, we found that as the radius increases, the aberration decreases, and that the optimal radius is 50 μm due to the dramatic drop of. Mie scattering increases as the microsphere radius increases. Our optimal radius based on spherical aberration, 50 μm, occurs before the relationship becomes exponential, indicating that our chosen radius remains valid. We performed durability calculations and found that the polyurethane adhesive tensile and compressive strength exceed those which will be induced on it during normal wear and tear. We chose polyurethane to bind the microspheres to the polyester for its temperature and adhesion properties. As a way to keep the

microspheres oriented for retroreflection throughout the application process, we used a polyimide adhesive film due to its weak adhesion properties.

Conclusions

Throughout the course of this project, our thought process shifted. The designs at the beginning and end of the course are significantly different from each other. As we gained more knowledge on both the materials and processes that would allow us to create a successful design, we found better options. At one point, we were considering using silane to increase the adhesion of the polyurethane, but we soon realized this was unnecessary after networking in the department. We set out to design a retroreflecting adhesive in order for a driver to see a pedestrian, based off of our angle of divergence calculations, this would be possible. We calculated that the reflectance for different incident angles and saw that the reflectance varies with angle, however, light will always be coming in at multiple angles and hitting many microspheres so this still allows for retroreflectivity to work in the manner with which we aimed for.

The materials we chose to use in our design include some of the same materials that are currently used in retroreflecting fabrics. Coated glass microspheres, like our choice of aluminum coated BaTiO_3 , are a well-known retroreflecting material. Current products available tend to be pressure sensitive adhesives, whereas ours is a hot-melt adhesive. In addition to the adhesive properties possible using a polyurethane hot-melt, we chose this type application in hopes that this method would give a more natural look to the clothing since the microspheres would essentially be implanted into the pores in the polyester fabric. The pressure sensitive tapes on the other hand sit on top of the fabric.

Future Work

Had this project been completed over a longer period of time, our team would have gone through with prototyping experiments and testing. Our prototyping would have started by fabricating our design. Tests would have been carried out on the product to test its retroreflective properties, namely the retroreflecting intensity in ambient light versus headlight conditions. Once we were satisfied with the performance, we would have assembled the product the way we intend our consumers to do so. Additional tests would have been completed to ensure the assembly process did not affect the retroreflectivity of the tape. Finally, we would have tested the durability and lifetime integrity of the tape while attached to clothing. Our original plan for prototyping only included designing and testing for the tape to be attached to polyester, although if given more time we would test other fabrics as well.

If we were to move forward, we have a clear path for future work. We would first need to find a better method of connecting all our ray tracing and aberration calculations to find the optimal radius. We would need to factor in intensities, which we had previously not done. We also should do our ray tracing at multiple wavelengths to represent the different colors of visible light. We would also look further into chromatic aberration and search for data about an index of refraction of 1.93 specifically or try to experimentally fit the Sellmeier Equation to 1.93 ourselves. After we completed the

project, we were made aware of some potential problems. One of them being that would we would need to consider the likelihood of our temporary polyimide adhesive will leave a residue. Since at this point in the process, the customer would be in possession of the product, we would need to find a simple and safe way for them to remove this residue. We would begin by physically prototyping the design to allow us to optimize the fabrication procedure. Testing of the selected polyurethane hot melt adhesive will allow us to confirm the reported properties, which will allow us to tune the fabrication process to maximize product quality. Further testing of the optical properties will ensure the retroreflective properties are maintained following the fabrication process. We will also begin application and durability testing of the tape to determine user experience, durability on additional types of clothing, product lifetime and degradation mechanisms.

Acknowledgements

We would like to thank Dr. Raymond Phaneuf for his guidance and support throughout the duration of this course as well as his assistance with the ray tracing modeling. We would also like to thank Drew Stasak's QUEST business project colleagues, specifically QUEST Professor J. Gerald Suarez, as well as teammates Laura Bell, Robert Crumbaugh, Donald Rutigliano, and Linda Yau. We would like to credit the original idea of a general reflective material to Donald Rutigliano. We would like to thank Dr. Robert Briber with his assistance with polymer properties and, for the brief time we considered its use, his help with silane properties. Finally, we would like to thank Christopher Wong for his advice on the use of silane.

References

- [1] *Traffic Safety Facts 2013 Data—Pedestrians*. National Highway Traffic Safety Administration, National Center for Statistics and Analysis, 2013.
- [2] Lloyd, John. "A Brief History of Retroreflective Sign Face Sheet Materials." *Understanding Retroreflectivity*. 2008.
- [3] Charles, Edwin Searight, Mclaurin Alexander Ezra, and Robert Ryan John. "High titanate glass beads." U.S. Patent No. 3,293,051. 20 Dec. 1966.
- [4] O'Bannon, Loran. "Dictionary of Ceramic Science and Engineering." New York: Plenum Press, 1983.
- [5] GLUETEX. *Technical Data Sheet UKF 438*. Klettgau-Erzingen: GLUETEX, 2015.
- [6] Leverette, Mary. "Are You Using The Right Iron Temperature?" *About.com*. About Home, 15 Dec. 2015.
- [7] 3M Electronics Materials Solutions Division, *3M™ Polyimide Film Tape 5413*, Saint Paul, Minnesota, 3M, 2014

- [8] Huelke, Donald F. "An Overview of Anatomical Considerations of Infants and Children in the Adult World of Automobile Safety Design." *Association for the Advancement of Automotive Medicine*. 42 (1998) 93-113.
- [9] United States of America. Virginia General Assembly. *Code of Virginia*.
- [10] Center for Disease Control and Prevention. "Anthropometric Reference Data for Children and Adults: United States, 2007-2010." *Vital and Health Statistics*, 11.252 (2012).
- [11] Budnik, Eric A., Carol C.Flannagan, Michael J. Flannagan, Shinichi Kojima, Michael Sivak. "The Locations of Headlamps and Driver Eye Positions in Vehicles in the U.S.A." *University of Michigan Transportation Research Institute*. Nov 1996.
- [12] Grabowski, Jurek G., Bethany D. Koetje. "A Methodology for the Geometric Standardization of Vehicle Hoods to Compare Real-World Pedestrian Crashes." *Association for the Advancement of Automotive Crashes*. 52 (2008) 193-198.
- [13] Koehler, Kenneth R. "Spectral Sensitivity of the Eye." *College Physics for Students of Biology and Chemistry*. 1996.
- [14] Nave, R. "Rod Details." *Hyperphysics*.
- [15] Alexander I. Lvovsky . Fresnel Equations. In Encyclopedia of Optical Engineering. Taylor and Francis: New York, Published online: 27 Feb 2013; 1-6.
- [16] Leng, Y. *Materials Characterization : Introduction to Microscopic and Spectroscopic Methods*. Second edition. Weinheim, Germany: Wiley-VCH, 2013. 7.Print.
- [17] Setzler, S. D., et al. "Periodically Poled Barium Titanate as a New Nonlinear Optical Material." *Advanced Solid State Lasers*. Optical Society of America, 1999.
- [18] Sacek, Vladimir. "Aberration Function." *Aberration Function*. N.p., 14 July 2006.
- [19] García-Cámara, B 'ON LIGHT SCATTERING BY NANOPARTICLES WITH CONVENTIONAL AND NON-CONVENTIONAL OPTICAL PROPERTIES' Diss. Universidad de Cantabria, 2010.
- [20] *Legislators Call on FDA to Study use of Plastic Microbeads in Toothpastes*. Regulatory Affairs Professionals Society, 2014.
- [21] Aguilera, Vicente, Kyösti Kontturi, Lasse Murtomäki, and Patricio Ramírez. "Estimation of the Pore Size and Charge Density in Human Cadaver Skin." *Journal of Controlled Release* 32.3 (1994): 249-57.